Detector-Free Fiber-Based Bidirectional Symmetric Communication Scheme Based on Compound States of Two Mutually Coupled Discrete-Mode Lasers

Andreas Herdt,[1] Markus Weidmann,[1] Adonis Bogris,[2] Richard Phelan,[3] and Wolfgang Elsäßer[1,4,5,*]

[1] *Institute of Applied Physics, Technische Universität Darmstadt, Schlossgartenstraße 7, 64289 Darmstadt, Germany*

[2] *Department of Informatics and Computer Engineering, University of West Attica, Aghiou Spiridonos, Egaleo, 12243 Athens, Greece*

[3] *Eblana Photonics Ltd, 3 West Pier Business Campus, Dun Laoghaire, Co. Dublin A96 A621, Ireland*

[4] *Also with: School of Physics, Trinity College Dublin, Dublin 2, Ireland*

[5] *Associated with Istituto di elettronica e di ingegneria dell'informazione e delle telecomunicazioni (IEIIT) del Consiglio Nazionale delle Richerche (CNR), Politecnico di Torino, Italy*

(Received 18 November 2023; accepted 10 January 2024; published 25 January 2024)

Most modern high-data-rate optical communication systems require at each end a light source to transmit the data and a detector to receive the data. In order to realize a communication scheme where the transmitter unites with the receiver, we take advantage of a coupled injection-locked semiconduct. From the theoretical description of two mutually coupled diode lasers using a set of six nonlinear differential-delay equations we outline the stable compound cavity solutions of this system and investigate their dependencies in terms of locking bandwidth, coupling strength and coupling phase. From these modeling results we then design a remarkably simple communication system without any additional detectors that exploits compound laser states of different frequency detunings of the coupled laser system as information carriers with simultaneous upstream information of the first laser and downstream information of the second laser. The data recognition is accomplished by evaluating the compound state utilizing the change in the terminal voltage of both lasers (laser-as-detector principle) with respect to their solitary case (i.e., the terminal voltage of the uncoupled lasers), yielding the message via the agreed decoding scheme. The functionality of the principle had been demonstrated by a table-top experiment with good error-free transmission and potential to improve the transmission speed of this proof-of-principle demonstration. Our concept reduces the complexity compared to conventional transmission systems, thus providing the potential to significantly reduce the costs of the overall transmission setup an,d in particular, transferring the concept to other challenging wavelengths and other semiconductor lasers. Since the optical signal then no longer needs to be detected by an optical detection unit, the amount of optical components required for ordinary data transmission is reduced.

DOI: 10.1103/PhysRevApplied.21.014049

I. INTRODUCTION

With the onset of the digital revolution humans began to exchange a huge amount of information utilizing digital telecommunication systems. Today, this data exchange occurs mainly via the internet, which developed from the military ARPANET in 1982 [1]. Since then data traffic has grown exponentially. At the beginning of 2020 around 177 exabytes of information were transferred via the internet per month, and the amount is still growing significantly every year [2]. The structure of the internet can be described as a huge weblike network, where computers are connected to other computers via big data nodes. The fastest and most energy-efficient connections are realized by optical interconnects and can transfer 283 terabits per second via a single transmission line [3]. A transmission line usually consists of optical transmitters at the sender position and optical receivers at the recipient position, while an optical fiber is used as the transport medium [4]. To extend this type of common transmission line for bidirectional communication, a second set of transmitters and receivers has to be deployed, where the former sender and recipient swap roles. However, this type of bidirectional communication requires only a single transport medium (i.e., the fiber), whereas at least two optical transmitters and two receivers are needed.

In order to reduce the number of optical components, we realize a bidirectional communication scheme where the transmitter unites with the receiver in a single optoelectronic element without introducing additional

*corresponding author. elsaesser@physik.tu-darmstadt.de

components in the setup, thus exploiting the laser-as-detector concept. Hence, for the transmission line only two combined transmitter/receiver units and one transport medium are required. To achieve this we take advantage of two delay-coupled 1550-nm discrete-mode (DM) semiconductor lasers [5], which are connected via a polarization-maintaining optical fiber.

By unidirectional injection of light from the first laser, now referred to as the master, into the second, verifying that both emit on similar wavelengths , a phenomenon called optical injection locking occurs [6–8]. The injected laser, now referred to as the slave, locks onto the optical wavelength of the master laser, and the frequency and amplitude characteristics of the master laser are transferred to the slave laser. This phenomenon is usually applied for frequency-stabilizing and modulating a powerful slave laser using a weak master laser [9]. Injection locking can also be used to synchronize the output of the master laser to a so-called twin laser [10–14]. Twin lasers share most of their optoelectronic properties. In particular, semiconductor twin lasers originate usually from the same wafer, and when operated alone they show similar output in amplitude and frequency as well as similar power consumption. Synchronization enables applications such as unidirectional [15] and bidirectional [16] secure chaos-communication systems, which have recently garnered renewed interest for application in the mid-infrared [17,18]. The fundamental idea of that application is to hide a message with a small amplitude within a chaotic signal of the transmitter such that the message does not disturb the larger chaotic fluctuations and remains camouflaged from an eavesdropper [19]. The injection-locked receiver (i.e., the slave) synchronizes only on the chaos and not on the message. By subtracting the slave signal from the master signal the message can be finally reconstructed. Nevertheless, this bidirectional chaos-communication scheme, presented in [16], has hitherto required at least four optical detectors, as with traditional communication systems.

When two diode lasers (DLs) are mutually delay-coupled and emit on similar wavelengths both of them become mutually injection-locked or, as we will henceforth say, mutually coupled. In that case, both lasers begin operation on an identical, time-independent frequency—the mutually coupled laser system operates on a so-called compound laser state (CLS) [20]. There is still a lack of investigation of appropriate applications for CLSs, and as yet only the emission stability and dynamics of these states have been reported [21–24].

Semiconductor lasers have the advantage that their frequency and amplitude can be controlled very well, so that different types of CLSs can be easily created and manipulated. In this contribution we exploit the CLSs of two mutually delay-coupled semiconductor lasers as data carriers for the bidirectional symmetric communication scheme presented here.

To finally evaluate and decode the CLSs we utilize the laser-as-detector principle [25–27], where we take advantage of a change in the terminal voltage due to the changes of the population inversion when operating on a CLS. This technique has been deployed in other applications, which are most commonly based on self-mixing [28], including spectroscopy [29–31], imaging [32] and the measurement of fundamental semiconductor laser properties [33,34], but has never been used for mutually coupled lasers for the purpose of data transmission. In our experiment, the laser-as-detector technique enables data transmission without any additional optical detector or element, finally reducing the number of optical components and thus the total costs of the system.

II. COMPOUND LASER STATES

Compound laser states represent the basis for the communication technique presented here. They can be generated by mutually delay-coupling two DLs emitting on similar wavelengths . A set of two mutually coupled DLs, DL-A and DL-B, can be theoretically described by a set of six nonlinear delay-coupled rate equations for the electrical field amplitude E_i, the electrical field phase ϕ_i, and the population inversion ΔN_i, with $i \in [A, B]$, following [35,36], where the subscripts A and B distinguish between DL-A and DL-B, respectively:

$$\frac{d\Delta N_A(t)}{dt} = \frac{\zeta J}{e} - \frac{\Delta N_A(t)}{\tau_{\text{eff}}} - g_A \cdot \Delta N_A(t) \cdot E_A^*(t) E_A(t), \tag{1}$$

$$\frac{dE_A(t)}{dt} = \left(g_A \cdot \Delta N_A - \frac{1}{\tau_{\text{ph}}}\right) E_A(t) + \left|\kappa_{\text{inj}}\right| E_B(t-\tau) E_A(t) \cdot \cos\left(\theta_{\text{inj}} + (\phi_B(t-\tau) - \phi_A(t)) + 2\pi\left(\Delta\nu t - \nu_A \tau\right)\right), \tag{2}$$

$$\frac{d\phi_A(t)}{dt} = \frac{\alpha}{2}\left(g_A \cdot \Delta N_A - \frac{1}{\tau_{\text{ph}}}\right) + \left|\kappa_{\text{inj}}\right| \frac{E_B(t-\tau)}{E_A(t)} \cdot \sin\left(\theta_{\text{inj}} + (\phi_B(t-\tau) - \phi_A(t)) + 2\pi\left(\Delta\nu t + \nu_A \tau\right)\right), \tag{3}$$

$$\frac{d\Delta N_B(t)}{dt} = \frac{\zeta J}{e} - \frac{\Delta N_B(t)}{\tau_{\text{eff}}} - g_B \cdot \Delta N_B(t) \cdot E_B^*(t) E_B(t), \tag{4}$$

$$\frac{dE_B(t)}{dt} = \left(g_B \cdot \Delta N_B - \frac{1}{\tau_{\text{ph}}}\right) E_B(t) + \left|\kappa_{\text{inj}}\right| E_A(t-\tau) E_B(t) \cdot \cos\left(\theta_{\text{inj}} + (\phi_A(t-\tau) - \phi_B(t)) - 2\pi\left(\Delta\nu t - \nu_B \tau\right)\right), \tag{5}$$

$$\frac{d\phi_B(t)}{dt} = \frac{\alpha}{2}\left(g_B \cdot \Delta N_B - \frac{1}{\tau_{\rm ph}}\right) + |\kappa_{\rm inj}|\frac{E_A(t-\tau)}{E_B(t)} \cdot \sin\left(\theta_{\rm inj} + (\phi_A(t-\tau) - \phi_B(t)) - 2\pi(\Delta\nu t + \nu_B\tau)\right). \quad (6)$$

Equations (1)–(3) describe the operation of DL-A and Eqs. (4)–(6) describe that of DL-B. The most important parameter responsible for the locking dynamics in general [6–14] is the so-called alpha parameter α defined as the quotient of the derivative of the imaginary part of the refractive index, the gain g with respect to the carrier density N, and the derivative of the real part of refractive index n with respect to N,

$$\alpha = \frac{dg/dN}{dn/dN}. \quad (7)$$

The parameter e denotes the elementary charge 1.602×10^{-19} C, J the carrier injection current density, and ζ the corresponding current injection efficiency. The characteristic times of the system are given by the effective carrier lifetime $\tau_{\rm eff}$, as well as the photon lifetime in the laser resonator $\tau_{\rm ph}$. The delay $\tau \equiv 2L/c$ describes the temporal distance between the DLs, which are spatially separated by the length L. The difference in the laser wavelengths λ_A and λ_B is usually converted to a difference in the optical frequencies, which is referred to as optical frequency detuning, described by the term $\Delta\nu$. It is defined as

$$\Delta\nu \equiv \nu_A^{\rm solitary} - \nu_B^{\rm solitary} = c \cdot \left(\frac{1}{\lambda_A} - \frac{1}{\lambda_B}\right). \quad (8)$$

Here, c denotes the speed of light and $\nu_A^{\rm solitary}, \nu_B^{\rm solitary}$ represent the optical frequencies of the uncoupled DL-A and DL-B, respectively.

The coupling coefficients $|\kappa_{\rm inj}|$ and $\theta_{\rm inj}$ are given by

$$|\kappa_{\rm inj}| = \tau^{-1} \cdot |T|, \quad (9)$$

$$\theta_{\rm inj} = 2\pi\Delta\nu \cdot \tau + \arg(T). \quad (10)$$

The complex term T contains all changes in the electrical field amplitude and phase passing the coupling path and includes changes caused by the injection into the secondary diode itself.

When the two solitary operating DLs, originally emitting on two similar optical frequencies ν_A and ν_B, experience mutual injection, they lock onto a joint optical frequency, which we now refer to as $\nu_{\rm CLS}$. In particular, the detuning $\Delta\nu$ (before injection locking occurs) must stay in a specific region, the so- called locking bandwidth (LBW) [20]. The maximal detuning, where frequency locking still occurs, defines the edges of this LBW and can be retrieved by an evaluation of the steady-state solutions of the coupled laser systems. It can be found that the width of the LBW $\Omega_{\rm LBW}$ is affected by the coupling strength $\kappa_{\rm inj}$, the coupling phase $\theta_{\rm inj}$, and the linewidth enhancement factor α of the DLs. In agreement with [20] for weakly coupled symmetrically pumped and identical lasers well above threshold the LBW, $\Omega_{\rm LBW}$ is given by

$$\Omega_{\rm LBW} = 2|\kappa_{\rm inj}|\sqrt{1+\alpha^2} \cdot |\cos(\arg(T) + 2\pi\,\nu_{\rm CLS}\tau + \arctan(\alpha))|. \quad (11)$$

Within the LBW the solutions of the rate equations [Eqs. (1)–(6)] are given by the CLSs, which are symbolically written as

$$\begin{aligned} \Delta N_A(t) &= \Delta N_{A,\rm CLS}, \\ S_A(t) &= S_{A,\rm CLS}, \\ \phi_A(t) &= 2\pi\,\nu_{\rm CLS}t, \\ \Delta N_B(t) &= \Delta N_{B,\rm CLS}, \\ S_B(t) &= S_{B,\rm CLS}, \\ \phi_B(t) &= 2\pi\,\nu_{\rm CLS}t + \sigma, \end{aligned} \quad (12)$$

where $\Delta N_{i,\rm CLS}$, $S_{i,\rm CLS}$, $\phi_{i,\rm CLS}$, $\nu_{\rm CLS}$, and σ are real-valued and $S_{i,\rm CLS} > 0$ with $i \in [A,B]$. Since the output power of a laser S is a more convenient quantity in experiments, the electrical field amplitude E has here been substituted by the optical power S via $E = \sqrt{S}$. The variable σ denotes a constant arbitrary time-independent phase shift between the lasers. Note that

$$\nu_{\rm CLS} = \nu_{i,j}^{\rm solitary} + \frac{1}{4\pi}\alpha_{i,j}\,g_{i,j}\,N_{i,j} \pm \frac{|\kappa_{\rm inj}|}{2\pi}\sqrt{\frac{S_{j,i}}{S_{i,j}}}\sin\left(\theta_{\rm inj} + \phi_{ji}\right). \quad (13)$$

where the plus sign is valid for the first subscript (laser A) and the minus sign for the second subscript (laser B), respectively, yielding one common expression for the frequency of the CLS $\nu_{\rm CLS}$. Here $\phi_{ji} \equiv \phi_j - \phi_i$ represents the phase difference of the electrical fields of lasers with $i,j \in [A,B]$, respectively. The variable $\nu_i^{\rm solitary}$ is the original optical frequency of the lasers in solitary operation.

Inside the LBW the photon emission S_i, the optical frequency ν_i, and most importantly the population inversion N_i change with respect to their solitary condition. The quantities are fully specified by the detuning $\Delta\nu$, the coupling coefficients $\kappa_{\rm inj}$ and $\theta_{\rm inj}$, where the latter are determined by the complex transmission coefficient T and the spatial distance L.

For a more intuitive representation, we now describe a CLS as follows:

$$\Gamma_{\rm CLS} \equiv (S_A, S_B, \Delta N_A, \Delta N_B, \Delta\nu), \quad (14)$$

where we assume a constant coupling strength and phase. With that knowledge, we find that the creation of a CLS

is quite simple. It only requires two mutually coupled DLs operating on two optical frequencies, which are separated within the range of the LBW and avoid too strong a coupling strength. In our communication approach we look for deterministic behavior and therefore we avoid high injection strengths, which are known to cause undesirable nondeterministic high-dimensional emission dynamics (e.g., chaos [37]). In the regime where we intend the coupled diode lasers to operate, they operate on stable so-called CLSs, also often referred to as compound laser modes in other literature [20].

III. IDENTIFICATION OF A COMPOUND LASER STATE: THE LASER-AS-DETECTOR PRINCIPLE

The identification of a CLS is as simple as its creation and is possible even without an additional optical detector. The laser-as-detector principle can be exploited, where the voltage change due to changes in the carrier density can be utilized, which occur due to changes in the quasi-Fermi level of the diode [25].

A good approximation for the voltage at a diode is given by the differences in the quasi-Fermi levels of electrons E_F^e and holes E_F^h and is given by

$$e \cdot U = E_F^e - E_F^h, \tag{15}$$

where e is the elementary charge. A change in the quasi-Fermi-level energies therefore results in a voltage change

$$e\Delta U = \Delta E_F^{h,e} \equiv \Delta E_F^e - \Delta E_F^h. \tag{16}$$

It is known that the quasi-Fermi levels are related to the carrier density. Assuming small changes compared to the actual carrier density, we can apply the first-order approximation

$$e\Delta U = B(N)\Delta N \tag{17}$$

with

$$B(N) \equiv \frac{1}{e}\frac{dE_F^{e,h}}{dN}. \tag{18}$$

where $E_F^{e,h}$ are the quasi-Fermi levels of the electrons and holes, respectively [26]. For typical DLs it has been found that the relation $(dE_F^{e,h})/dN$ is a positive function [25].

According to Eqs. (17) and (18), it can be concluded that a change in the population inversion ΔN in the case of mutual coupling is transferred to a change of terminal voltage at the DL. Although this voltage change is small (usually a few millivolts) compared to the original terminal voltage of the laser, it is still high enough to be detected reliably.

Now that we have a theoretical framework for the creation and identification of a CLS, we can proceed with a description of the experimental implementation in the next sections for communication purposes.

IV. EXPERIMENTAL SETUP

In order to experimentally create a CLS, the proposed scheme takes advantage of the easy wavelength control of the utilized DLs. In discrete-mode DLs the optical frequency (i.e., the wavelength) is controlled by the injected current. The relation between current I and optical frequency ν_i of our twin-DM DLs is found by a calibration with an optical spectrum analyzer and results in

$$\nu_A^{\text{solitary}}(I) = -1.38\,\frac{\text{GHz}}{\text{mA}} \cdot I + 194.349\,\text{THz}. \tag{19}$$

$$\nu_B^{\text{solitary}}(I) = -1.39\,\frac{\text{GHz}}{\text{mA}} \cdot I + 194.349\,\text{THz}, \tag{20}$$

for DL-A and DL-B, respectively. By mutually coupling these two DLs a CLS with any desired relative detuning can be created using the tunable current sources which are synchronized by a common clock generator. The setup for mutual coupling is schematically depicted in Fig. 1, where the coupling path is visualized in red, passing several optical components.

The setup also contains the electrical devices for the identification of a CLS. For that purpose two conventional dc voltmeters measure the terminal voltage changes at each DL. An exemplary trace of the terminal voltage changes of both DLs for a wide range of detunings is visualized in Fig. 2 (red and blue) together with the LBW (green). To obtain this graph, we measure the terminal voltages of both DLs when ν_A is scanned across the fixed optical frequency of DL-B via current tuning. The optical frequency

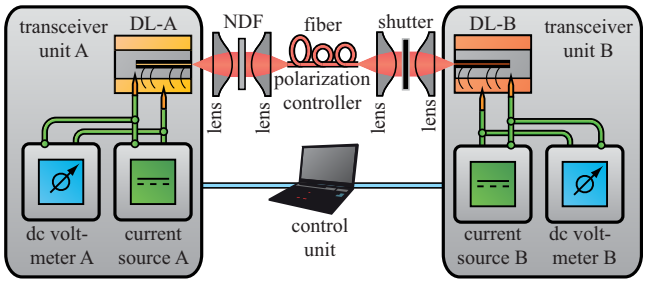

FIG. 1. Schematic experimental setup showing the mutually coupled discrete mode DLs with receiver-transmitter (transceiver) units (grey boxes), coupling/communication path (red), and control unit. The transceiver units each contain a DL, a current source and a dc voltmeter. The coupling path includes several lenses, a neutral density filter (NDF) to control the injection strength, a fiber with a polarization controller in order to provide matching of the polarization, as well as a shutter so that the lasers' terminal voltage can be determined in solitary uncoupled operation case. A clock generator between the two current sources was used to ensure the synchronization of the data transfer.

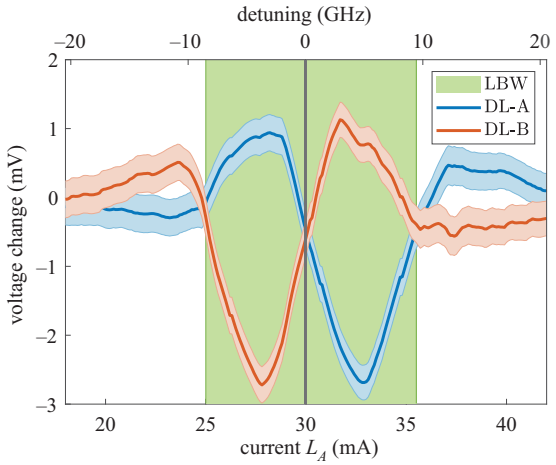

FIG. 2. Voltage change with measurement uncertainties (shaded color border), when the optical frequency ν_A of DL-A is scanned across a fixed optical frequency of DL-B. The vertical grey line marks the fixed current $I_B = 30$ mA of DL-B indicating its fixed solitary optical frequency which is $\nu_B = 1.9431$ THz. The upper detuning x-axis is obtained by reference measurements of the optical spectrum of each laser operating solitarily. The green area visualizes the locking bandwidth Ω_{LB}.

of DL-B is set to $\nu_B = 194\,307.3$ GHz, by providing a constant current [38]. We keep the coupling phase constant by keeping the distance fixed and also provide a constant coupling strength $|\kappa_{\mathrm{inj}}|$. We perform a reference measurement of the terminal voltages with closed shutter (compare Fig. 1), so both lasers operate in solitary mode. This reference measurement and the actual measurement of the terminal voltages of the coupled lasers allow for calculating the voltage change which is finally displayed for both lasers in Fig. 2.

The detuning axis (Fig. 2, top) is obtained by the frequency difference

$$\Delta\nu = \nu_A(I)^{\mathrm{solitary}} - \nu_B^{\mathrm{solitary}}. \tag{21}$$

It is obvious that the change in the terminal voltage of DL-A is opposed to that of DL-B with a zero crossing at $\Delta\nu = 0$ GHz. This type of calibration measurement enables us to detect the signum of $\Delta\nu$, provided that $\Delta\nu \in \Omega_{\mathrm{LBW}}$ only by the terminal voltage of each DL. If, for example, the terminal voltage of DL-B decreases with respect to its solitary value, then the injected optical frequency of DL-A must be smaller: $\nu_{\mathrm{A}}^{\mathrm{solitary}} < \nu_B^{\mathrm{solitary}}$. When no voltage change is observed, both lasers must operate on the same frequency: $\nu_{\mathrm{A}}^{\mathrm{solitary}} = \nu_B^{\mathrm{solitary}}$. If the voltage of DL-B is increased with respect to its solitary value, then the injected optical frequency must be higher: $\nu_{\mathrm{A}}^{\mathrm{solitary}} > \nu_B^{\mathrm{solitary}}$. This dependency holds also when interchanging DL-A with DL-B (i.e., interchanging subscripts A and B in the previous equations).

In conclusion, we find that the voltage change is perfectly suited to determine the original detuning of both lasers and thus identify different CLSs. This remarkable feature enables using the CLSs to carry information. The process of encoding data onto CLSs and decoding CLSs back to bits is discussed in the following section.

V. DATA ENCODING AND DECODING AND THE COMMUNICATION PROTOCOL

For a complete bidirectional communication it is required to make sure that transferring all possible bit combinations (00), (01), (10), and (11) is possible. These bit combinations are now referred to as compound bits. The first digit of a compound bit represents the bit transferred by DL-A and the second digit the bit transferred by DL-B, respectively. The compound bits are encoded onto four different CLSs ($\Gamma_{00}, \Gamma_{01}, \Gamma_{10}$, and Γ_{11}), which serve as the data carriers. In order to create these four states we utilize two different frequencies ν_0 and $\nu_1 > \nu_0$, ensuring $\nu_1 - \nu_0 \in \Omega_{\mathrm{LBW}}$:

$$\Gamma_{00} = \left(S_A^{00}, S_B^{00}, \Delta N_A^{00}, \Delta N_B^{00}, \Delta\nu = 0\right) \text{ with } (\nu_A = \nu_B = \nu_0), \tag{22}$$

$$\Gamma_{01} = \left(S_A^{01}, S_B^{01}, \Delta N_A^{01}, \Delta N_B^{01}, \Delta\nu = \nu_1 - \nu_0\right) \text{ with } (\nu_A = \nu_1,\ \nu_B = \nu_0), \tag{23}$$

$$\Gamma_{10} = \left(S_A^{10}, S_B^{10}, \Delta N_A^{10}, \Delta N_B^{10}, \Delta\nu = \nu_0 - \nu_1\right) \text{ with } (\nu_A = \nu_0,\ \nu_B = \nu_1), \tag{24}$$

$$\Gamma_{11} = \left(S_A^{11}, S_B^{11}, \Delta N_A^{11}, \Delta N_B^{11}, \Delta\nu = 0\right) \text{ with } (\nu_A = \nu_B = \nu_1). \tag{25}$$

It can be seen that both Γ_{00} and Γ_{11} yield a detuning of $\Delta\nu = 0$ resulting in a voltage change of the DLs close to zero (as shown in Fig. 2). The compound bits (01) and (10) represent a nonzero detuning $\Delta\nu \neq 0$ and the corresponding voltage change in both lasers is nonzero. For a better overview of the compound bits, the optical frequencies ν_i and the resulting voltage changes are summarized in Table I. It will later be clear that the identification of the

TABLE I. Compound bits and the corresponding optical frequencies ν_A and ν_B, which result in the voltage changes. Vc DL-A, voltage change in DL-A compared to solitary reference; Vc DL-B, voltage change in DL-B compared to solitary reference.

DL-A sends	DL-B sends	Compound bit	Opt. freq. ν_A	Opt. freq. ν_B	Vc DL-A	Vc DL-B
0	0	(00)	ν_0	ν_0	~ 0	~ 0
0	1	(01)	ν_0	ν_1	$\neq 0$	$\neq 0$
1	0	(10)	ν_1	ν_0	$\neq 0$	$\neq 0$
1	1	(11)	ν_1	ν_1	~ 0	~ 0

TABLE II. Decoding table resembling a XOR gate, which holds for both transceiver units. Tx, own transferred bit; Vc, voltage change recognized, yes = 1, no = 0; Rx, received bit.

Tx	Vc	Rx
0	0	0
0	1	1
1	0	1
1	1	0

CLSs does not require a measurement of the signum of the voltage change in order to decode the compound bit.

Now that it is known how the previously defined compound bits affect the voltages of both lasers, a tool to decode the compound bit at each transceiver unit is needed in order to finally decode the message sent by the secondary unit. This decoding scheme holds for both transceiver units and takes advantage of those voltage changes as well as of the self-knowledge of the optical frequency. The decoding table follows a logical exclusive-or gate (XOR gate) with its own transferred bit as an argument and its own recognized voltage change as the second argument and is presented in Table II and holds for both transceiver units.

With these tools for experimental encoding and decoding data utilizing CLSs, it is possible to simultaneously transfer data from one transceiver unit to the other. We present a demonstration data communication in the following section.

VI. DEMONSTRATION DATA COMMUNICATION AND COMMUNICATION PROTOCOL

Figure 1 schematically depicts the experimental setup, which is used for demonstrating data communication exploiting mutually coupled 1550-nm discrete mode DLs. The DLs are independently driven by a constant current source (ILX LDX 3232). The terminal voltages are individually measured by two external voltmeters (Keithley Multimeter 2400). The coupling path, 2.25 m long (2 m fiber, 0.25 m air), contains a neutral density filter (NDF) to fine-tune the coupling strength such that the injection-locked DLs operate in a stable regime. For reference measurements the integrated shutter allows disconnecting the coupling path to measure the dc voltage in solitary mode. With the polarization controller integrated into the 2-m fiber path, this enables each incident light polarization to match the outgoing polarization of both lasers' radiation. Using that setup, we transfer the first letters "TUD" (abbreviation for "Technische Universität Darmstadt") from transceiver unit A to transceiver unit B and "hlo" (abbreviation for the German name of the working group, "Halbleiteroptik") in the opposite direction. For that purpose we apply the following communication protocol:

(1) Define letters to be transmitted. We choose "TUD" from transceiver unit A to transceiver unit B and "hlo" in the opposite direction.

(2) Each control unit encodes its message to be transferred into a series of bits using the UTF-8 format. In UTF-8 format, letters are represented by a sequence of 8 bits. The string "TUD" for example is represented by the sequence "01010100|01010101|01000100" and "hlo" by "01101000|01101100|01101111".

(2b) We begin the transfer with the first bidirectional bit (00) transferring a "0" bit from transceiver unit A to transceiver unit B and also a "0" in the opposite direction.

(3) We switch the optical frequency ν of each DL by current-switching to either ν_0 or ν_1 according to the bit values defined in (2) (cf. Table I). In our demonstration experiment, a bit representing a "0" is transferred by switching the optical frequency to $\nu_1 = 194\,307.3$ GHz (1542.88 nm), a bit representing a "1" by switching to $\nu_0 = 194\,303.825$ GHz (1542.91 nm).

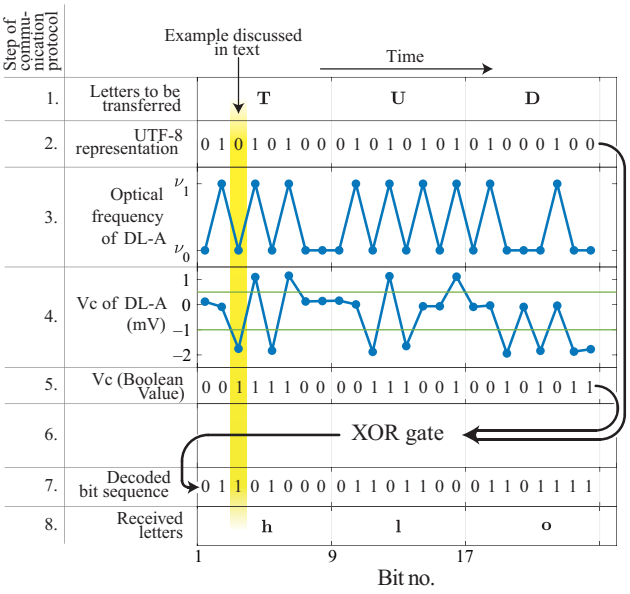

FIG. 3. Visualized procedure of the communication protocol (top to bottom) at transceiver unit B. The letters "TUD" are transferred from transceiver unit A to transceiver unit B. In step 2 the letters "TUD" are represented by their UTF-8 representation. In step 3 the optical frequency of DL-A is shown according to Table I. The values of the recognized voltage changes (Vc) at transceiver unit A are depicted in step 4. The green lines indicate the thresholds when a voltage change is considered to be equal to zero or unequal to zero. In between the thresholds a voltage change is considered to be equal to zero; above or below both lines it is considered to be nonzero. The resulting Boolean value is shown in step 5. The logical XOR gate (step 6) yields the received bit (step 7) and the full message can be deciphered by converting the whole bit sequence into letters again using the UTF-8 format (step 8). The received word from transceiver unit B is "hlo".

(4) The voltage changes V_c are observed at each DL individually by the dc voltmeters.

(5) These observed voltage changes V_c are transferred to Boolean bit values considering the defined threshold border values.

(6) The logical XOR gate is applied onto the bits transferred in (2) and registered in (5).

(7) The logical XOR gate yields the received bit (cf. Table II).

(7b) Steps (2)–(7) are repeated until the messages have been fully transferred in both directions.

(8) Finally, we obtain the received messages at each transceiver unit by converting the full bit sequences obtained in (7) into letter strings by decoding them using the UTF-8 format.

The process of the communication protocol is visualized along the example transmission in Figs. 3 and 4, where each line represents a step of the protocol. As an example

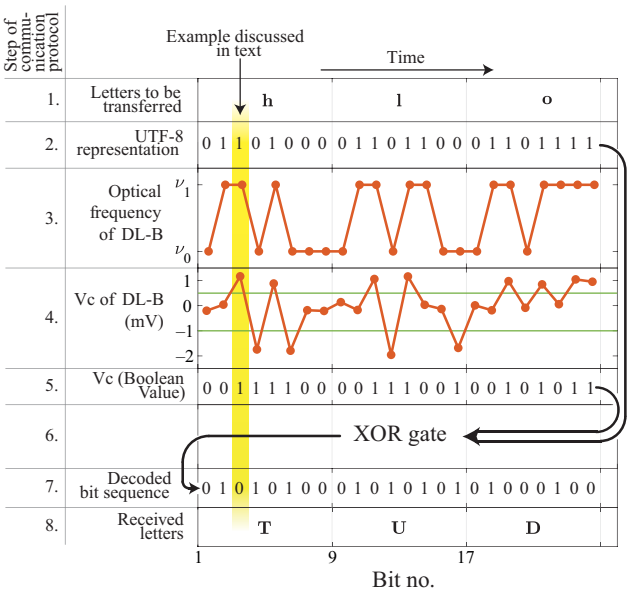

FIG. 4. Visualized procedure of the communication protocol (top to bottom) at transceiver unit B. The letters "hlo" are transferred from transceiver unit B to transceiver unit A. In step 2 the letters "hlo" are represented by their UTF-8 representation. In step 3 the optical frequency of DL-B is shown according to Table I. The values of the recognized voltage changes (Vc) at transceiver unit B are depicted in step 4. The green lines indicate the thresholds, when a voltage change is considered to be equal to zero or unequal to zero. In between the thresholds a voltage change is considered to be equal to zero; above or below both lines it is considered to be nonzero. The resulting Boolean value is shown in step 5. The logical XOR gate (step 6) yields the received bit (step 7) and the full message can be deciphered by converting the whole bit sequence into letters again using the UTF-8 format (step 8). The received word from transceiver unit A is "TUD".

of steps (2)–(7) we consider the transfer of the bidirectional bit (01), which is highlighted in Figs. 3 and 4 with a vertical yellow bar. In that case, transceiver unit A sends a "0" bit, while transceiver unit B sends a "1" bit at the same time. The optical frequency of DL-A is therefore set to ν_0 via current tuning and that of DL-B to ν_1. This yields a detuning of $\Delta\nu = \nu_0 - \nu_1 \neq 0$. In agreement with Table I, this scenario leads to a nonzero voltage change at each DL. The terminal voltage of DL-A increases by 1 mV and that of DL-B decreases by 2 mV, which can be seen in Fig. 3 (middle graph) and Fig. 4 (middle graph), respectively. For decoding, transceiver unit A inserts its own sent bit "0" and the recognized voltage change "1" into the XOR gate (Table II) and decodes the received bit to be "1". For decoding, transceiver B inserts its own sent bit "1" and the recognized voltage change "1" into the same XOR gate and decodes the received bit to be "0".

VII. DISCUSSION I: TRANSMISSION SPEED AND ROBUSTNESS OF THE SCHEME

We find that the transfer scheme performs remarkably well and each bit of the demonstration transfer as seen in Figs. 3 and 4 has been decoded without error. However, at the moment the system is only capable of transferring messages of equal length of each side. The transmission speed of our proof-of-concept setup as described performs at an average bit rate of 1.3 B/s.

The transmission speed in our present experimentally realized case is only limited by the control unit and not by physical processes. However, it can be significantly increased until its physical limitation is reached, which is given the time it takes to establish a CLS. This time ultimately depends on the lasers used and their internal parameters, such as the response time of the lasers as well as the distance, which in our case is of the order of 10 ns. Beside that low transmission speed, we proved the reliability of that system in terms of bit-error rate to be very good. It was possible to demonstrate a transmission of 5800 bits within a continuous transmission of random compound bits over a period of 2.1 h. In total we obtained 43 wrongly decoded compound bits, resulting in a bit-error rate of $43/5800 = 7.4 \cdot 10^{-3}$. Errors occur when the terminal voltage does not correctly change above/below the agreed-upon threshold, which can for example be caused by electrical perturbation from the current source (the agreed upon thresholds of the demonstration transmission are depicted by the green lines in Figs. 3 and 4). The approach also provides detection of a disconnection by statistics. In the case of a disconnection event each transceiver would recognize a zero voltage change for every bit it is transmitting. Since for very large data transfers the probability of the compound bits (10) and (01) is statistically the same as the probability for (11) and (00), the disconnection can then be recognized when the equilibrium shifts significantly.

With that we have successfully shown the first demonstration of a data transmission without additional optical detectors utilizing two mutually coupled DLs operating on CLSs within a laser-as-detector approach. Additionally, the approach even offers further potential with respect to data-rate improvement and privacy, which we briefly discuss in the next section.

VIII. DISCUSSION II: FURTHER POTENTIALS OF THE SCHEME

Even though already very promising, the scheme demonstrated offers further potential. On the one hand it is possible to significantly increase the data rate, while on the other hand the scheme also provides potential for camouflaging the data transfer.

The data rate can, for example, be increased using wavelength multiplexing. We have already stated that at large detunings, which are far away from the LBW, two mutually coupled DLs do not interact with each other. Hence, the detection of a CLS is selective with respect to the optical frequency. Considering this, the approach provides the potential to use the same fiber for various optical frequencies spaced by more than a few LBWs. No additional wavelength multi- and demultiplexing units are required.

Apart from high-speed data transmission, secure exchange of information is currently an important and challenging topic for the significantly increasing amount of data transferred around the world's communication networks. Communication schemes based on quantum cryptography have been developed [39,40], which ensure security due to the no-cloning theorem of quantum mechanics. Two important transmission protocols for quantum communication are the BB84 [41] and Ekert [42] protocols, which have been implemented for free space [43], satellite-based [44], and fiber-based [45] communication. Another security-enhanced transfer scheme, chaos communication, is based on high-dimensional dynamics and coherence collapse of laser-light subjected to self-feedback [46,47]. In this communication scheme two lasers operating in the chaotic regime are unidirectionally coupled and the synchronization between them allows for the extraction of the information that has been camouflaged in the chaotic emission [48,49]. Apart from chaos communication, the so-called ghost-polarization communication [50] enables security-enhanced information exchange by exploiting hidden polarization states. The latter can only be recovered by the receiver using a second-order correlation analysis. The scheme demonstrated in this work, based on mutually coupled DLs, automatically provides a basic level of privacy, but compared to the previously mentioned secure transmission methods based on classical light, the technique presented here does not require complex setups and is therefore technically very simple to deploy. In our scheme the decoding always requires the knowledge of the sent bit (cf. Table II). Thus, a hypothetical eavesdropper could not easily decode the message. It is assumed that an eavesdropper only has access to the optical signals S_A and S_B in the coupling path as well as to the optical frequency ν_{CLS}. The fundamental reflection symmetry of the mutually coupled laser rate equation system [20] is described by

$$(S_A, S_B, N_A, N_B, \Delta\nu) \rightarrow (S_B, S_A, N_B, N_A, -\Delta\nu)\,. \tag{26}$$

Together with Eq. (13) this yields for our scheme that the compound bits (01) and (10) are not distinguishable using the common optical frequency ν_{CLS} without the knowledge of the sent bit. Thus, the message transfer is considered to be obscured from the eavesdropper, which is a highly advantageous intrinsic feature of our remarkably simple setup. However, other potential attack vectors, including transient analysis [51] or man-in-the-middle attacks [52], need to be considered in further investigations.

IX. SUMMARY

We have successfully demonstrated a bidirectional symmetric fiber-communication scheme based on two mutually coupled 1550-nm discrete-mode diode lasers without an additional optical detection unit. Within this approach, we exploited the laser-as-detector approach to decode and receive bits using the terminal voltage changes, when both lasers emit on a common compound laser state. This proof-of-concept shows a remarkable reliability demonstrated by an error-free transmission of more than 5800 bits. Since the scheme is very economical with regard to optical components and does not require additional optical detection units, the system reduces the complexity compared to conventional transmission systems, thus providing the potential to significantly reduce the costs of the overall transmission setup. Beside the reduction of optical components, the proof-of-concept still offers exceptional potential with regard to an improvement in transmission speed, which can be significantly increased until its physical limitation is reached, which is given the time it takes to establish a CLS and enhancement in privacy, which all need to be evaluated in further investigations. Last, but certainly not less interesting, is the fact that the scheme is not limited to the twin 1550 nm lasers utilized. By using other types of semiconductor laser pairs, such as quantum cascade and interband cascade lasers, this proof of-principle experiment can be transferred to other wavelengths, where detectors are expensive, slow or even not available, such as the mid-infrared or the terahertz region, with even the potential for offering bidirectional communication in free space.

ACKNOWLEDGMENTS

The authors thank D. Auth and C. Weber for fruitful and stimulating discussions. We acknowledge support by M.

Rosskopf in completing the manuscript. We thank Prof. D. Lenstra for discussions about dynamics of compound laser states.

[1] Barry M. Leiner, Vinton G. Cerf, David D. Clark, Robert E. Kahn, Leonard Kleinrock, Daniel C. Lynch, Jon Postel, Larry G. Roberts, and Stephen Wolff, A brief history of the internet, ACM SIGCOMM Comput. Commun. Rev. **39**, 22 (2009).

[2] CISCO. Cisco Visual Networking Index: Forecast and Trends, 2017–2022 White Paper. 2019.

[3] Georg Rademacher, Ruben S. Luis, Benjamin J. Puttnam, Tobias A. Eriksson, Roland Ryf, Erik Agrell, Ryo Maruyama, Kazuhiko Aikawa, Yoshinari Awaji, Hideaki Furukawa, and Naoya Wada, High capacity transmission with few-mode fibers, J. Lightwave Technol. **37**, 425 (2019).

[4] Nathan Blaunstein, Shlomo Engelberg, Evgenii Krouk, and Mikhail Sergeev, *Fiber Optic and Atmospheric Optical Communication* (John Wiley & Sons, Hoboken NJ, 2019).

[5] L. P. Barry, C Herbert, D Jones, A Kaszubowska-Anandarajah, B Kelly, J O'Carroll, R Phelan, P Anandarajah, K Shi, and J O'Gorman, in *Novel In-Plane Semiconductor Lasers VIII* (International Society for Optics and Photonics SPIE, Bellingham WA, 2009), Vol. 7230, p. 72300N.

[6] Roy Lang, Injection locking properties of a semiconductor laser, IEEE J. Quantum Electron. **18**, 976 (1982).

[7] Soichi Kobayashi and Tatsuya Kimura, Injection locking characteristics of an algaas semiconductor laser, IEEE J. Quantum Electron. **16**, 915 (1980).

[8] Isabelle Petitbon, Philippe Gallion, Guy Debarge, and Claude Chabran, Locking bandwidth and relaxation oscillations of an injection-locked semiconductor laser, IEEE J. Quantum Electron. **24**, 148 (1988).

[9] F. Mogensen, H. Olesen, and G. Jacobsen, Locking conditions and stability properties for a semiconductor laser with external light injection, IEEE J. Quantum Electron. **21**, 784 (1985).

[10] Rajarshi Roy and K. Scott Thornburg Jr, Experimental synchronization of chaotic lasers, Phys. Rev. Lett. **72**, 2009 (1994).

[11] Michael Peil, Tilmann Heil, Ingo Fischer, and Wolfgang Elsäßer, Synchronization of chaotic semiconductor laser systems: a vectorial coupling-dependent scenario, Phys. Rev. Lett. **88**, 174101 (2002).

[12] H. J. Wünsche, S. Bauer, J. Kreissl, O. Ushakov, N. Korneyev, F. Henneberger, E. Wille, H. Erzgräber, M. Peil, W. Elsäßer, and I. Fischer, Synchronization of delay-coupled oscillators: A study of semiconductor lasers, Phys. Rev. Lett. **94**, 163901 (2005).

[13] Noam Gross, Wolfgang Kinzel, Ido Kanter, Michael Rosenbluh, and Lev Khaykovich, Synchronization of mutually versus unidirectionally coupled chaotic semiconductor lasers, Opt. Commun. **267**, 464 (2006).

[14] Thomas Jungling, Xavier Porte, Neus Oliver, Miguel C. Soriano, and Ingo Fischer, A unifying analysis of chaos synchronization and consistency in delay-coupled semiconductor lasers, IEEE J. Sel. Top. Quantum Electron. **25**, 1 (2019).

[15] Apostolos Argyris, Dimitris Syvridis, Laurent Larger, Valerio Annovazzi-Lodi, Pere Colet, Ingo Fischer, Jordi García-Ojalvo, Claudio R. Mirasso, Luis Pesquera, and K. Alan Shore, Chaos-based communications at high bit rates using commercial fibre-optic links, Nature **438**, 343 (2005).

[16] Raúl Vicente, Claudio R. Mirasso, and Ingo Fischer, Simultaneous bidirectional message transmission in a chaos-based communication scheme, Opt. Lett. **32**, 403–5 (2007).

[17] L. Jumpertz, F. Michel, R. Pawlus, Wolfgang Elsäßer, K. Schires, M. Carras, and F. Grillot, Measurements of the linewidth enhancement factor of mid-infrared quantum cascade lasers by different optical feedback techniques, AIP Adv. **6**, 015212 (2016).

[18] F. Grillot, O. Spitz, A. Herdt, W. Elsäßer, and M. Carras, in *Quantum Sensing and Nano Electronics and Photonics XVII* (International Society for Optics and Photonics SPIE, Bellingham WA, 2020), Vol. 11288, p. 112881P.

[19] Pere Colet and Rajarshi Roy, Digital communication with synchronized chaotic lasers, Opt. Lett. **19**, 2056 (1994).

[20] Hartmut Erzgräber, Bernd Krauskopf, and Daan Lenstra, Compound laser modes of mutually delay-coupled lasers, SIAM J. Appl. Dyn. Syst. **5**, 30 (2006).

[21] Eric Wille, Michael Peil, Ingo Fischer, and Wolfgang Elsäßer, Dynamical scenarios of mutually delay-coupled semiconductor lasers in the short coupling regime, Proc. SPIE **5452**, 41 (2004).

[22] F. Rogister and M. Blondel, Dynamics of two mutually delay-coupled semiconductor lasers, Opt. Commun. **239**, 173 (2004).

[23] H. Erzgräber, D. Lenstra, B. Krauskopf, E. Wille, M. Pzeil, Ingo Fischer, and Wolfgang Elsäßer, Mutually delay-coupled semiconductor lasers: Mode bifurcation scenarios, Opt. Commun. **255**, 286 (2005).

[24] Miguel C. Soriano, Jordi García-Ojalvo, Claudio R. Mirasso, and Ingo Fischer, Complex photonics: Dynamics and applications of delay-coupled semiconductors lasers, Rev. Mod. Phys. **85**, 421 (2013).

[25] Shuichi Mitsutsuka and Junichi Shimada, Voltage change across the self-coupled semiconductor laser, IEEE J. Quantum Electron. **17**, 1216 (1981).

[26] Silvano Donati, Responsivity and noise of self-mixing photodetection schemes, IEEE J. Quantum Electron. **47**, 1428 (2011).

[27] Andrew Grier, Paul Dean, Alexander Valavanis, James Keeley, Iman Kundu, Jonathan D. Cooper, Gary Agnew, Thomas Taimre, Yah Leng Lim, Karl Bertling, Aleksandar D. Rakić, Lianhe H. Li, Paul Harrison, Edmund H. Linfield, Zoran Ikonić, A. Giles Davies, and Dragan Indjin, Origin of terminal voltage variations due to self-mixing in terahertz frequency quantum cascade lasers, Opt. Express **24**, 21948 (2016).

[28] A. D. Rakić, T. Taimre, K. Bertling, Y. L. Lim, P. Dean, A. Valavanis, and D. Indjin, Sensing and imaging using laser feedback interferometry with quantum cascade lasers, Appl. Phys. Rev. **6**, 021320 (2019).

[29] Mark C. Phillips and Matthew S. Taubman, Intracavity sensing via compliance voltage in an external cavity quantum cascade laser, Opt. Lett. **37**, 2664 (2012).

[30] Mark C. Phillips, Matthew S. Taubman, and Jason Kriesel, in Manijeh Razeghi, Eric Tournié, and Gail J. Brown, editors, *Quantum Sensing and Nanophotonic Devices XII* (International Society for Optics and Photonics, SPIE, Bellingham WA, 2015), Vol. 9370, p. 192.

[31] Rabi Chhantyal-Pun, Alexander Valavanis, James T. Keeley, Pierluigi Rubino, Iman Kundu, Yingjun Han, Paul Dean, Lianhe Li, A. Giles Davies, and Edmund H. Linfield, Gas spectroscopy with integrated frequency monitoring through self-mixing in a terahertz quantum-cascade laser, Opt. Lett. **43**, 2225 (2018).

[32] Paul Dean, Alex Valavanis, James Keeley, Karl Bertling, Yah Leng Lim, Raed Alhathlool, Siddhant Chowdhury, Thomas Taimre, Lianhe H. Li, Dragan Indjin, Stephen J. Wilson, Aleksandar D. Rakić, Edmund H. Linfield, and A. Giles Davies, Coherent three-dimensional terahertz imaging through self-mixing in a quantum cascade laser, Appl. Phys. Lett. **103**, 181112 (2013).

[33] Yanguang Yu, Guido Giuliani, and Silvano Donati, Measurement of the linewidth enhancement factor of semiconductor lasers based on the optical feedback self-mixing effect, IEEE Photonics Technol. Lett. **16**, 990 (2004).

[34] Jens Von Staden, Tobias Gensty, Wolfgang Elsäßer, Guido Giuliani, Christian Mann, Wolfgang Elsäßer, Guido Giuliani, and Christian Mann, Measurements of the alpha factor of a distributed-feedback quantum cascade laser by an optical feedback self-mixing technique, Opt. Lett. **31**, 2574 (2006).

[35] Daan Lenstra, Self-consistent rate-equation theory of coupling in mutually injected semiconductor lasers. in Bernd Witzigmann, Marek Osiński, and Yasuhiko Arakawa, editors, *Proc. SPIE, 2017*, Vol. 10098, p. 100980K.

[36] Josep Mulet, Cristina Masoller, and Claudio R. Mirasso, Modeling bidirectionally coupled single-mode semiconductor lasers, Phys. Rev. A **65**, 063815 (2002).

[37] Tilmann Heil, Ingo Fischer, Wolfgang Elsässer, Josep Mulet, and Claudio R. Mirasso, Chaos synchronization and spontaneous symmetry-breaking in symmetrically delay-coupled semiconductor lasers, Phys. Rev. Lett. **86**, 795 (2001).

[38] The optical frequency of $\nu_B = 194307.3$ GHz represents a wavelength of $\lambda_B = 1542.88$ nm.

[39] Charles H. Bennett and Gilles Brassard, Quantum cryptography: Public key distribution and coin tossing, Theor. Comput. Sci. **560**, 7 (2014).

[40] Stefano Pirandola, End-to-end capacities of a quantum communication network, Commun. Phys. **2**, 1 (2019).

[41] C. H. Bennett and G. Brassard, Quantum cryptography: Public key distribution and coin tossing. *Proc. of IEEE Int. Conf. on Comput. Sys. and Sign. Proces*, (1984).

[42] Artur K. Ekert, Quantum cryptography based on Bell's theorem, Phys. Rev. Lett. **67**, 661 (1991).

[43] Thomas Jennewein, Christoph Simon, Gregor Weihs, Harald Weinfurter, and Anton Zeilinger, Quantum cryptography with entangled photons, Phys. Rev. Lett. **84**, 4729 (2000).

[44] Juan Yin, Yu-Huai Li, Sheng-Kai Liao, Meng Yang, Yuan Cao, Liang Zhang, Ji-Gang Ren, Wen-Qi Cai, Wei-Yue Liu, and Shuang-Lin Li *et al.*, Entanglement-based secure quantum cryptography over 1,120 kilometres, Nature **582**, 501 (2020).

[45] Boris Korzh, Charles Ci, Wen Lim, Raphael Houlmann, Nicolas Gisin, Ming Jun Li, Daniel Nolan, Bruno Sanguinetti, Rob Thew, and Hugo Zbinden, Provably secure and practical quantum key distribution over 307 km of optical fibre, Nat. Photonics **9**, 163 (2015).

[46] Marc Sciamanna and K. Alan Shore, Physics and applications of laser diode chaos, Nat. Photonics **9**, 151 (2015).

[47] Fabien Rogister, Alexandre Locquet, Didier Pieroux, Marc Sciamanna, Olivier Deparis, Patrice Mégret, and Michel Blondel, Secure communication scheme using chaotic laser diodes subject to incoherent optical feedback and incoherent optical injection, Opt. Lett. **26**, 1486 (2001).

[48] Gregory D. Vanwiggeren and Rajarshi Roy, Communication with chaotic lasers, Science **279**, 1198 (1998).

[49] C. Masoller, Anticipation in the synchronization of chaotic semiconductor lasers with optical feedback, Phys. Rev. Lett. **86**, 2782 (2001).

[50] Markus Rosskopf, Till Mohr, and Wolfgang Elsäßer, Ghost polarization communication, Phys. Rev. Appl. **13**, 034062 (2020).

[51] Avi Zadok, Jacob Scheuer, Jacob Sendowski, and Amnon Yariv, Secure key generation using an ultra-long fiber laser: Transient analysis and experiment, Opt. Express **16**, 16680 (2008).

[52] Keijo Haataja and Pekka Toivanen, Two practical man-in-the-middle attacks on bluetooth secure simple pairing and countermeasures, IEEE Trans. Wireless Commun. **9**, 384 (2010).